Density functional theory description of the mechanism of ferromagnetism in nitrogen-doped SnO_2

Run Long, Niall J. English

The SEC Strategic Research Cluster and the Centre for Synthesis and Chemical Biology, Conway Institute of Biomolecular and Biomedical Research, School of Chemical and Bioprocess Engineering, University College Dublin, Belfield, Dublin 4, Ireland.

Abstract: Based on first-principles calculations, we have studied the occurrence of spin polarization in the magnetic metal oxide SnO_2 doped with nonmagnetic nitrogen (N) impurities. It was found that the local magnetic moments are localized mainly on the N dopant, causing a total moment of $0.95\mu_B$ per cell. The long-range magnetic coupling of N-doped SnO_2 may be attributed to a *p-p* coupling interaction between the N impurity and host valence states.

Keywords: N dopant, SnO_2, ferromagnetic, coupling mechanism

1. Introduction

Dilute magnetic semiconductors (DMS) have attracted much attention due to their potential application in spintronics. Most previous studies have focused on magnetic 3d transition-metal (TM) doped DMS, based on group III-V and II-VI host materials [1, 2]. Recently, however, unexpected high-temperature ferromagnetism (FM) has been observed in a series of materials, which do not contain ions with partially filled *d* or *f* bands [3]; this has provoked a strong interest in investigating further the occurrence and nature of high-temperature ferromagnetism.

SnO_2 is a wide band-gap material which has been used as a transparent conducting electrode in solar cells [4] and gas sensors [5]. TM (Co, Fe, Cr, V, and Ni)-doped SnO_2 exhibits ferromagnetism above room temperature (RT) [6-10]. However, the origin of ferromagnetism observed in these different experiments is still under debate; Rahman et al. [11] have even showed that it is possible to induce magnetism in SnO_2 without doping of TM from first-principles. Recently, RT ferromagnetism was found in C-doped ZnO by replacement of O atoms by C atoms [12]. The group reported subsequently using first-principles calculations that N-doped ZnO can also display weak ferromagnetism [13]. Besides ZnO, Gu et al. [14] also reported that ferromagnetism was found in N-doped MgO within the tight-binding approximation and quantum Monte Carlo simulation. It would appear that the phenomenon of d^0 ferromagnetism may be a distinct possibility in a range of metal oxidies.

In the present work, we have studied the electronic structure and magnetic properties of N-doped SnO_2 by density functional theory (DFT) calculations for a series of N-doped configurations. The calculated results show that each N atom induces a magnetic moment of $0.95\mu_B$ per cell and the N dopants tend to substitute the neighboring anions and favor FM spin-ordering. Long-range RT ferromagnetic behavior was found to be associated with holes mediated through *p-p* interaction between the impurities and host atoms. We corroborated this finding further by examination of the spatial spin distribution.

2. Methodology

All of the spin-polarized DFT calculations were performed using the projector augmented wave (PAW) pseudopotentials, as implemented in the VASP code [15, 16]. The Perdew and Wang parametrization [17] of the generalized gradient approximation [18] was adopted for the exchange-correlation potential. The electron wave function was expanded in plane waves up to a cutoff energy of 400 eV and a Monkhorst–Pack *k*-point mesh [19] of 4 × 4 × 4 was used for a (2 × 2 × 2) 48-atom rutile SnO_2 supercell for geometry optimization and electronic property calculations. The cell and atomic relaxations were carried out until the residual forces were below 0.01 eV/Å. The optimized lattice parameters were $a = b = 4.764$ Å and $c = 3.221$Å, in good agreement with experimental values [20].

3. Results and Discussion

3.1 Local magnetic order

Replacement of a single O atom by one N atom (N@O) in the supercell corresponds to a 2.08 % N concentration. N@O favors a spin-polarized state and its total energy is 439 meV lower than that of nonspin-polarized states, indicating thereby that the ground state of N-doped SnO_2 is stable. Each N impurity introduces a total magnetic moment of $0.95\mu_B$ per cell, composed of $\sim 0.72\mu_B$ from N itself, $\sim 0.14\mu_B$ from its nearest-neighboring O atoms and $\sim 0.09\mu_B$ from its next nearest-neighboring Sn atoms. In essence, the substitution of an O atom by an N atom leads to a spontaneous magnetization of N inside SnO_2. The calculated total density (DOS) and projected DOS (PDOS) of 2p states of N, of the nearest-neighboring O atoms and of the 3d states of one of the next nearest-neighboring Sn atoms, are shown in Figures 1a & b, respectively. As shown in Figure 1, the N 2p states are distributed mainly in the valence band due to the hybridization with O 2p states, leaving unoccupied ghost states in the forbidden gap. Figure 1 shows also that N 2p states overlap slightly with O 2p and Sn 3d states above the Fermi level, E_F, resulting in an obvious splitting above E_F. The corresponding spin-density distribution is shown in Figure 3(a). It shows clearly that the spin density in N-doped SnO_2 is localized mainly on the N atom and distributed slightly on its eight nearest-neighboring O atoms and the three first-neighboring Sn atoms. This means that magnetic orbital coupling extends to the nearest-neighboring O atoms from the N dopant center. Therefore, anions from the delocalized p orbitals contribute chiefly to the magnetic moment in N-doped SnO_2.

3.2 Long-rang magnetic order

To examine long-range magnetic coupling of magnetic moments in N-doped SnO_2, we considered eight different configurations of two-N-atom anion doped SnO_2, corresponding to a dopant concentration of 4.2%. For convenience, the replaced oxygen atoms have been marked with numbers 0-8 in Figure 1. The eight structures were obtained by two N atoms substituting two O atoms at (0, 1), (0, 2), (0, 3), (0, 4), (0, 5), (0, 6), (0, 7), and (0, 8) with different N-N distances, respectively.

Table 1 lists the energy difference between FM and anti-ferromagnetic(AFM) spin-ordering and the magnetic moments of these eight dopant configurations. The energy difference between the FM state and AFM state ($\Delta E = E(FM) - E(AFM)$) spin-ordering indicates the lowest one to be the ground-state magnetic ordering. The calculated results show that the magnetic moments of the two N dopants favor significantly the FM state in the (0, 1) configuration, and the energy of the FM state is 43 meV lower than that of the corresponding AFM state. Its magnetic moments increased to 1.90 μ_B, twice than that of single N-doped SnO_2, which agrees well with our above discussion about N dopant-induced magnetism. This indicates also that the most remarkable coupling is rather strong for the shortest N-N distance of 2.616Å. This suggests a “cluster effect” of N dopants in the supercell, which is quite distinct from transition metal-doped SnO_2 [7, 8]. Figures 3(b) (cf. FM state) show the spin density between the two N ions separated by 2.616 Å in the (0, 1) configuration. Figure 3(a) shows that the nearest-neighbor O atoms of N atoms mediate the magnetic

coupling. Furthermore, the charge carriers localized around the O between these N ions are polarized and have same spin orientation as that of N ions. Consequently, these polarized charge carriers facilitate the long-range ferromagnetic coupling between the N ions. This suggests that the holes mediate the mechanism of ferromagnetic coupling in N-doped SnO_2.

It should be noted that the valence DOS of the SnO_2 is dominated by O 2p states, whereas the bottom of the unoccupied conduction band consists mainly of Sn 4s, 4p and O 2p antibonding states. Replacement of one O atom with one N atom introduces holes in the O 2p states in the valence band, which couples with the N 2p localized spins by a *p-p* interaction, similar to *p-d* hybridization in TM-doped semiconductors. This *p-p* interaction leads to the appearance of new mixed states in the band gap. The coupling was found to result in spin-splitting with the majority of *p-p* spin states downwards. The spatial extension of *p* states of the host and impurity atoms were found to extend *p-p* interactions and spin alignment to a large range and thus to facilitate long-range magnetic coupling between the two N impurities.

Finally, we discuss briefly the exchange interaction in N-doped SnO_2 based on the PDOS of N 2px, 2py, and 2pz, as shown in Figure 4. Near E_F, the N 2py and N 2pz states are spin-polarized due to a hybridization interaction with O 2p states, while the N 2px state has slight contribution due to lying in a deeper energy region. Only a minority of N 2py orbitals consist of spin-down empty states, so hybridization between occupied N 2px, 2py, 2pz and O2p states with empty N 2py states leads to an exchange interaction. Therefore, hybridization between the N 2p states and O 2p

states leads to stable ferromagnetism.

4. Conclusions

To summarize, we have studied N anion doped SnO2 with density functional theory calculations. It has been shown that N impurities acquire magnetization with a magnetic moment of $0.95\mu_B$ due to the fully empty N 2p states located in the band gap. The long-rang ferromagnetic coupling between two N dopants is through *p-p* interaction in this N-doped SnO_2 material.

Acknowledgements

This work was supported by the Irish Research Council for Science, Engineering and Technology (IRCSET). The authors acknowledge Science Foundation Ireland and the Irish Centre for High-End Computing for the provision of computational facilities.

References

[1] H. Ohno, Science 281 (1998) 951.

[2] T. Dietl, H. Ohno, F. Matsukura, J. Cibert, and D. Ferrand, Science 287 (2000) 1019.

[3] I. S. Elfimov, S. Yunoki, and G. A. Sawatzky, Phys. Rev. Lett. 89 (2002)216403.

[4] H. L. Hartnagel, A. L. Dewar, A. K. Jain, and C. Jagadish, Semiconducting Transparent Thin Films (IOP, Bristol, 1995)

[5] A. Vancu, R. Ionescu and N. Bârsan, Chemoresistive gas sensors. In: P. Ciureanu and S. Middelhoek Editors, Thin Film Resistive Sensors Institute of Physics Publishing, New York (1992).

[6] S. B. Ogale et al., Phys. Rev. Lett. 91 (2003) 077205.

[7] J. M. D. Coey, A. P. Douvalis, C. B. Fitzgerald, and M. Venkatesan, Appl. Phys. Lett. 84 (2004)1332.

[8] N. H. Hong, J. Sakai, W. Prellier, and A. Hassini, J. Phys.: Condens.Matter 17 (2005) 1697.

[9] N. H. Hong and J. Sakai, Physica B 358 (2005) 265.

[10] N. H. Hong, A. Ruyter, W. Prellier, J. Sakai, and N. T. Huong, J. Phys.: Condens. Matter 17 (2005) 6533.

[11] G. Rahman, V. M. García-Suárez, and S. C. Hong, Phys. Rev. B 78 (2008)184404.

[12] H. Pan, J. B. Yi, L. Shen, R. Q. Wu, J. H. Yang, J. Y. Lin, Y. P .Feng, J. Ding, L. H. Van, and J. H. Yin, Phys. Rev. Lett. 99 (2007) 127201.

[13] L. Shen, R. Q. Wu, H. Pan, G. W. Peng, M. Yang, Z. D. Sha, and Y. P. Feng, Phys. Rev. B 78 (2008) 073306.

[14] B. Gu, N. Bulut, T. Ziman, and S. Makekawa, Phys. Rev. B 79 (2009) 024407.

[15] G. Kresse, J. Hafner, Phys. Rev. B 47 (1994) 558.

[16] G. Kresse, J. Furthermüller, Phys. Rev. B 54 (1996)11169.

[17] J. P. Perdew, K. Burk, M. Ernzerhof, Phys. Rev. Lett. 77 (1996) 3865.

[18] J. P. Perdew, Y. Wang, Phys. Rev. B 45 (1992) 13244.

[19] H. J. Monkhorst, J. D. Pack, Phys. Rev. B 13 (1976) 5188.

[20] H. Matsuhata, J. Gjonnes, J. Tafto, Acta Cryst. A50 (1994) 115.

TABLE 1. Energy difference between FM and AFM spin-ordering ΔE= E(FM)-E(AFM)**,** magnetic moment of N ion M_N, and total magnetization of the supercell, M_{tot}, in its stable state (FM or AFM) for different N-N distances in the eight doping configurations N(i, j) (i=0, j= 1,8).

(i, j)	N-N(Å)	ΔE(meV)	$M_N(\mu_B)$	$M_{tot}(\mu_B)$
(0, 1)	2.616	-43	1.44	1.89
(0, 2)	2.924	22	0	0
(0, 3)	3.222	-4	1.44	1.89
(0, 4)	4.150	6	0	0
(0, 5)	4.764	-2	1.44	1.89
(0, 6)	5.116	0	0	0
(0, 7)	5.751	-16	1.44	1.89
(0, 8)	7.345	34	0	0

Figure Captions

Figure 1. 48-atom (2 × 2 × 2) supercell of rutile SnO_2 employed to define model B-doped SnO_2 structures. The large green and small red spheres represent the Sn and O atoms, respectively. The O atoms labeled by 0–8 are the sites to be replaced with N atoms.

Figure 2 (a) Total DOS of N-doped SnO_2 and (b) projected DOS for N 2p, the eight nearest-neighbor O 2p states and three nearest-neighbor Sn 4d orbitals. The Fermi level has been set to zero.

Figure 3 Spin density for (a) single N doping, (b) two N doping for an FM state separated by 2.616 Å. Yellow and green isosurfaces correspond to up- and down-spin densities, respectively.

Figure 4 PDOS for N 2px, N 2py, and N 2pz states. The Fermi level has been set to zero.

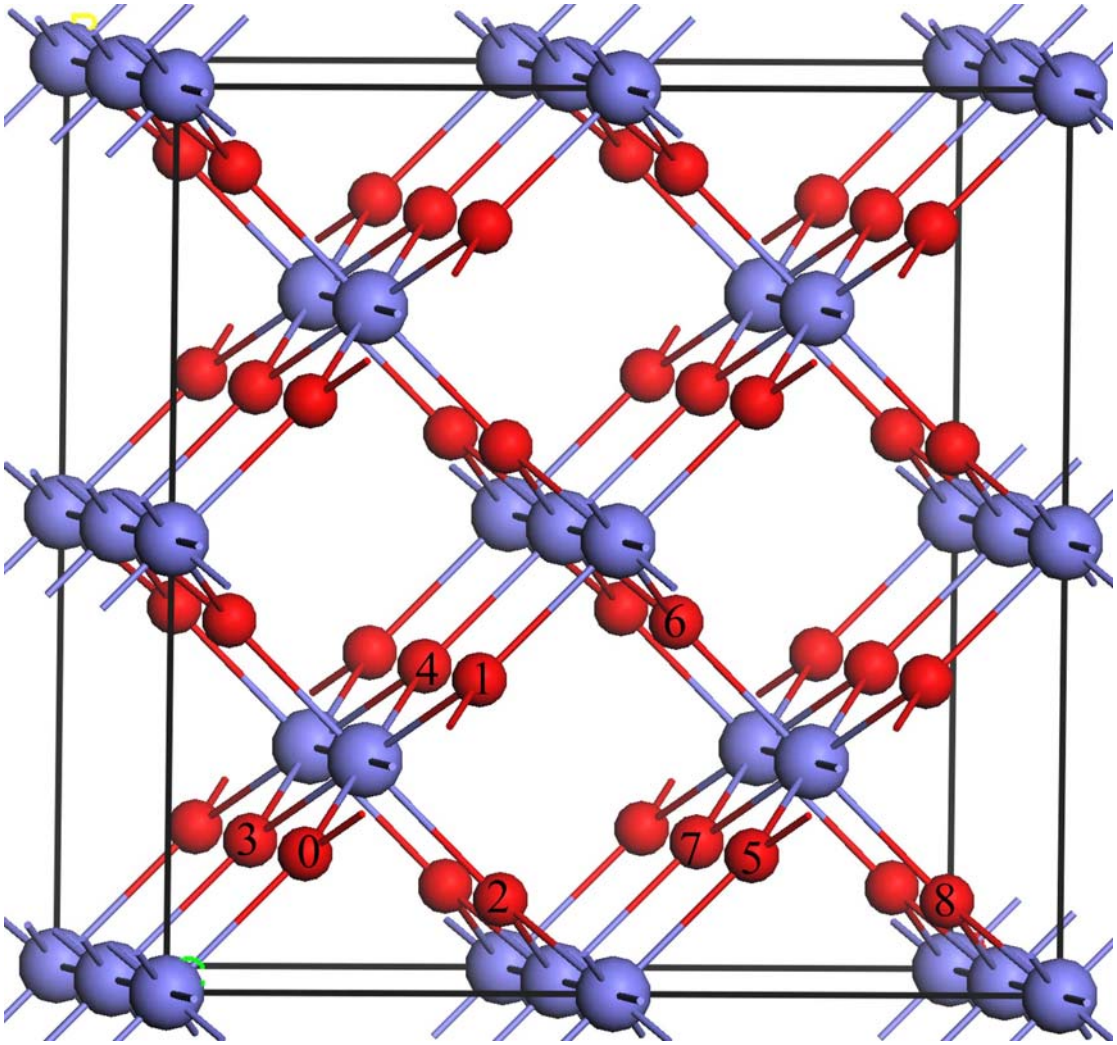

Figure 1

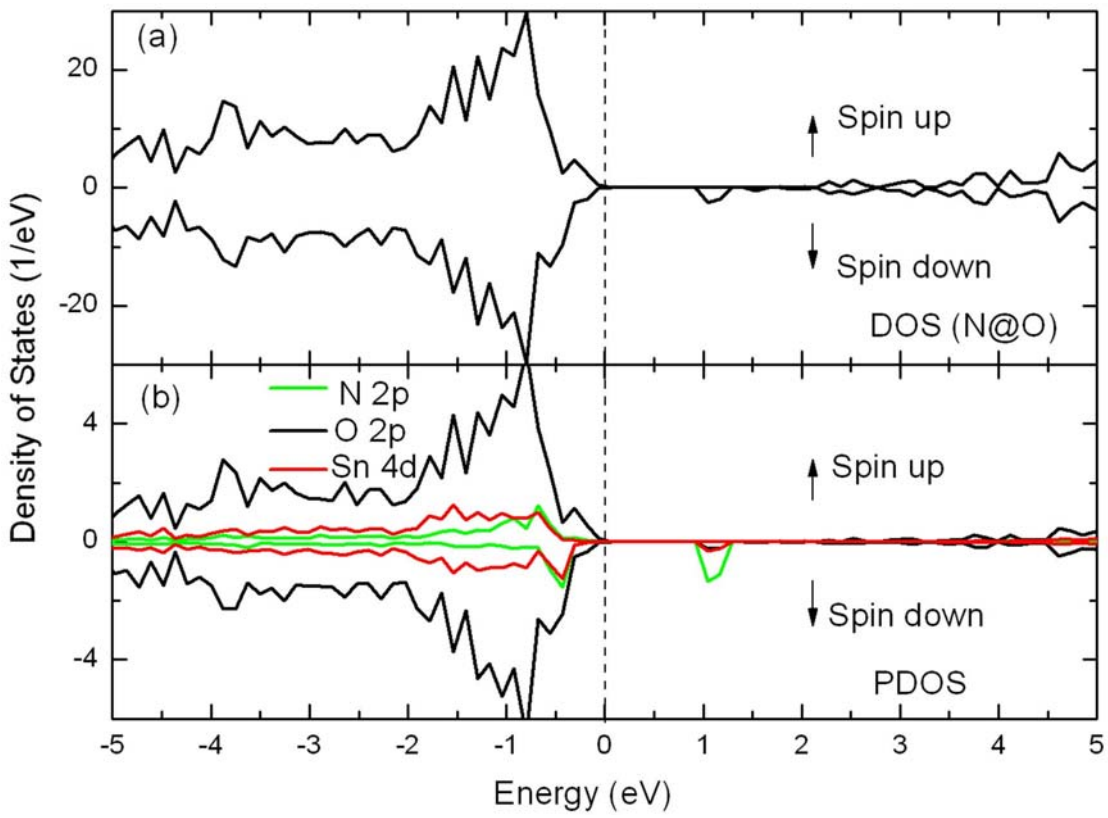
(a)
20
0
-20
Spin up
Spin down
DOS (N@O)
(b)
N 2p
O 2p
Sn 4d
4
0
-4
Spin up
Spin down
PDOS
Density of States (1/eV)
-5
-4
-3
-2
-1
0
1
2
3
4
5
Energy (eV)

Figure 2

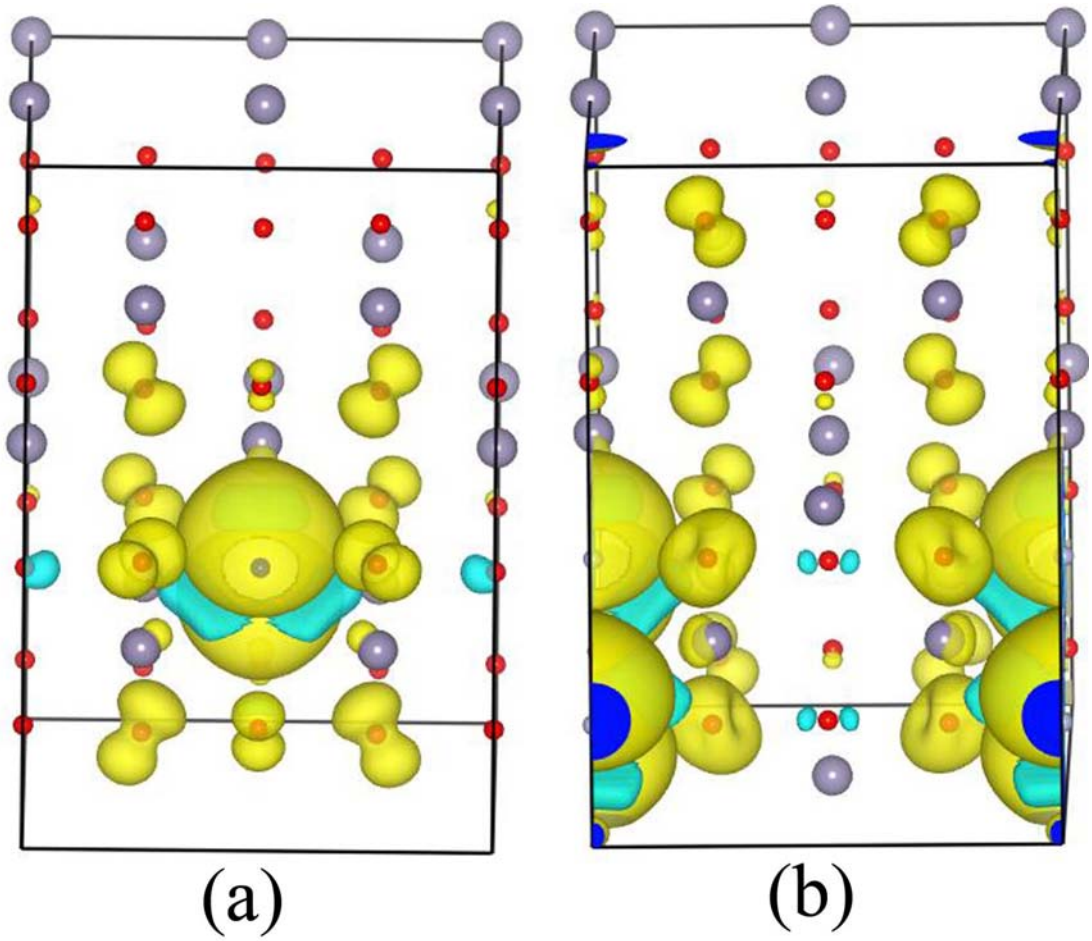

Figure 3

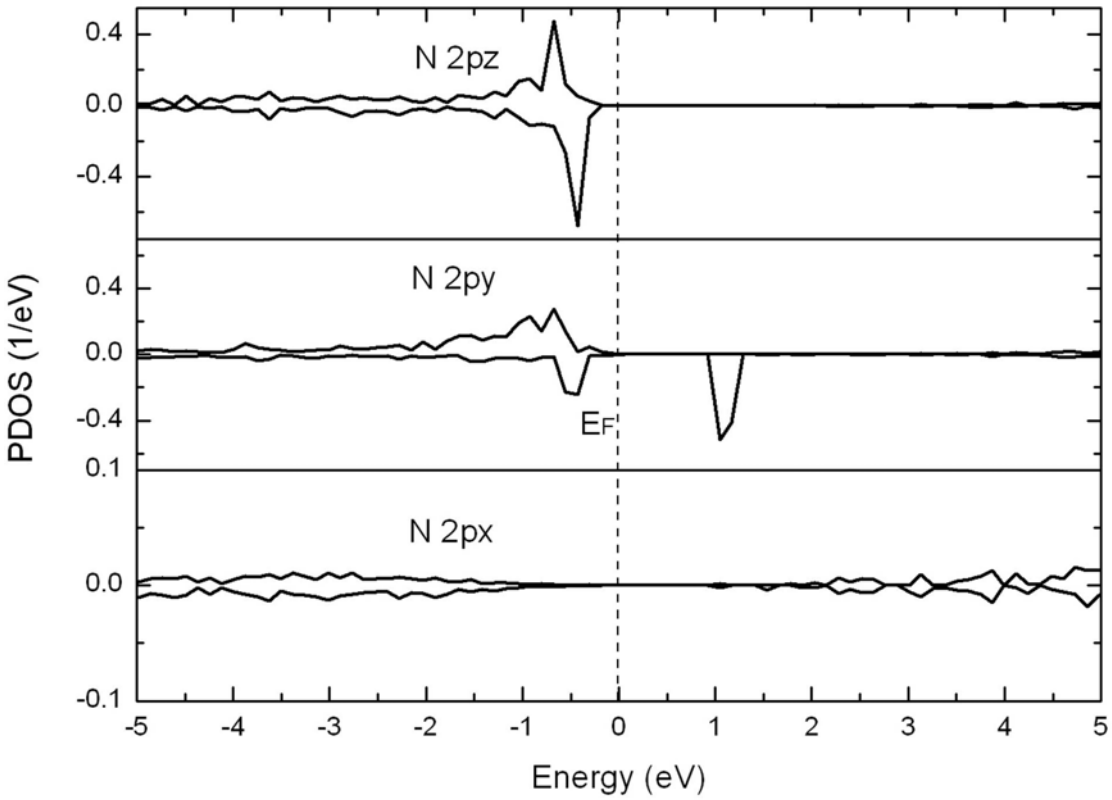
N 2pz
N 2py
N 2px
PDOS (1/eV)
Energy (eV)
E_F
0.4
0.0
-0.4
0.1
-0.1
-5
-4
-3
-2
-1
0
1
2
3
4
5

Figure 4